

# Single-cell RNA sequencing reveals cellular and molecular heterogeneity in fibrocartilaginous enthesis formation

Tao Zhang<sup>a, c, d\*</sup>, Wan Liyang<sup>a, c, d\*</sup>, Xiao Han<sup>a, c, d</sup>, Linfeng Wang<sup>a, c, d</sup>, Jianzhong Hu<sup>b, c, d</sup>, Hongbin Lu<sup>a, c, d</sup>

<sup>a</sup> Department of Sports Medicine, Xiangya Hospital, Central South University, Changsha 410008, China

<sup>b</sup> Department of Spine Surgery and Orthopaedics, Xiangya Hospital, Central South University, Changsha 410008, China

<sup>c</sup> Key Laboratory of Organ Injury, Aging and Regenerative Medicine of Hunan Province, Changsha 410008, China

<sup>d</sup> National Clinical Research Center for Geriatric Disorders, Xiangya Hospital, Central South University, Changsha 410008, China

**INTRODUCTION:** The attachment site of the rotator cuff (RC) is a classic fibrocartilaginous enthesis, which is the junction between bone and tendon with typical characteristics of a fibrocartilage transition zone. Enthesis development has historically been studied with lineage tracing of individual genes selected a priori, which does not allow for the determination of single-cell landscapes yielding mature cell types and tissues.

**METHODS:** Here, in together with open source GSE182997 datasets (3 sample) provided by Fang et al, we applied Single-cell RNA sequencing (scRNA-seq) to delineate the comprehensive postnatal RC enthesis growth and the temporal atlas from as early as postnatal day 1 up to postnatal week 8. And we furtherly performed single cell spatial transcriptomic sequencing on postnatal day 1 mice enthesis, in order to deconvoluted bone-tendon junction (BTJ) chondrocytes onto spatial spots.

**RESULTS SECTION:** So far, there is only one transcriptomic study for embryonic mouse enthesis has been carried out using single cell RNA sequencing (Kult et al., 2021). However, the development of fibrocartilage at the enthesis of mouse rotator cuffs occurs no earlier than 2 weeks after birth (Galatz et al., 2007), suggesting the investigation at postnatal stage of cellular and genomic mechanisms in enthesis development is needed. According to the works performed by Fang F et al. (Fang et al., 2022), they found enthesis progenitors (Gli1+ progenitors) and validated their stemness in-vitro and in-vivo, within the timepoints from P11 to P56. In this study, we applied single-cell transcriptome analysis to delineate the comprehensive postnatal enthesis growth with temporal atlas from as early as postnatal day 1 up to postnatal day 56. We next used the spatial transcriptome sequencing on postnatal day-1 mice enthesis to verify the anatomical position of different cell populations.

**DISCUSSION:** There are some certain limitations in the current study. Firstly, we could not remove all the humeral head cells because the enthesis tissues only contain 4-5 layers of cells and are located adjunct to bone marrow and growth plate. Future use of high-precision microdissection approaches to isolate region-specific cells will address the limitation. Secondly, it is undeniable that spatial transcriptomics are better reliable to address possible dissociation artifacts and gain spatial information. However, utilization of spatial transcriptomic sequencing on enthesis are limited owing to the difficulty in sectioning without decalcification, which restricted our attempt to acquire spatial transcriptomics on mature enthesis with tough bony tissue.

**SIGNIFICANCE/CLINICAL RELEVANCE:** (1-2 sentences): We deciphered the cellular heterogeneity and the molecular dynamics during fibrocartilage differentiation. Combined with current spatial transcriptomic data, our results provide a transcriptional resource that will support future investigations of enthesis development at the mechanistic level and may shed light on the strategies for enhanced RC healing outcomes.

**ACKNOWLEDGEMENTS:** The authors would like to thank professor Hui Xie, Xiang-Hang Luo and other staff from Movement System Injury and Repair Research Center, Xiangya Hospital, Central South University, Changsha, China, for their kind assistance during the experiments.

## IMAGES AND TABLES:

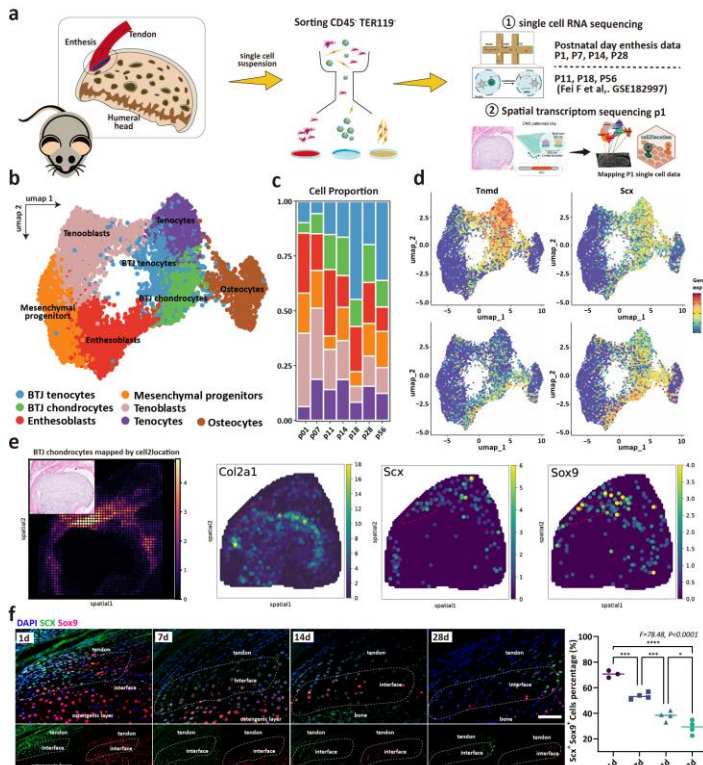


**Figure 1** Unbiased clustering identified Known Cell Populations in postnatal enthesis development. (A) Schematic workflow of the study design. (B) Distributions of 7 cell clusters on UMAP plot, including BTJ chondrocytes, BTJ tendons, tenocytes, osteocytes, enthesoblasts, tenoblasts, and mesenchymal

progenitors. (C) Fractions of cell clusters in enthesis development at P1, P7, P11, P14, P18, P28 and P56. (D) The average expression of curated feature genes for previously reported enthesis marker genes and enthesis-specific ECM genes. (E) Spatial transcriptomic spot map revealing the expression of chondrocyte marker genes in each spatial spot. (F) Representative immunofluorescence staining to validate the spatial distribution of Sox9+ and Scx+ cells in the enthesis area, at P1, P7, and P14. Scale bars, 100  $\mu$ m. \* =  $P < 0.05$ , \*\*\* =  $P < 0.001$ , \*\*\*\* =  $P < 0.0001$ .

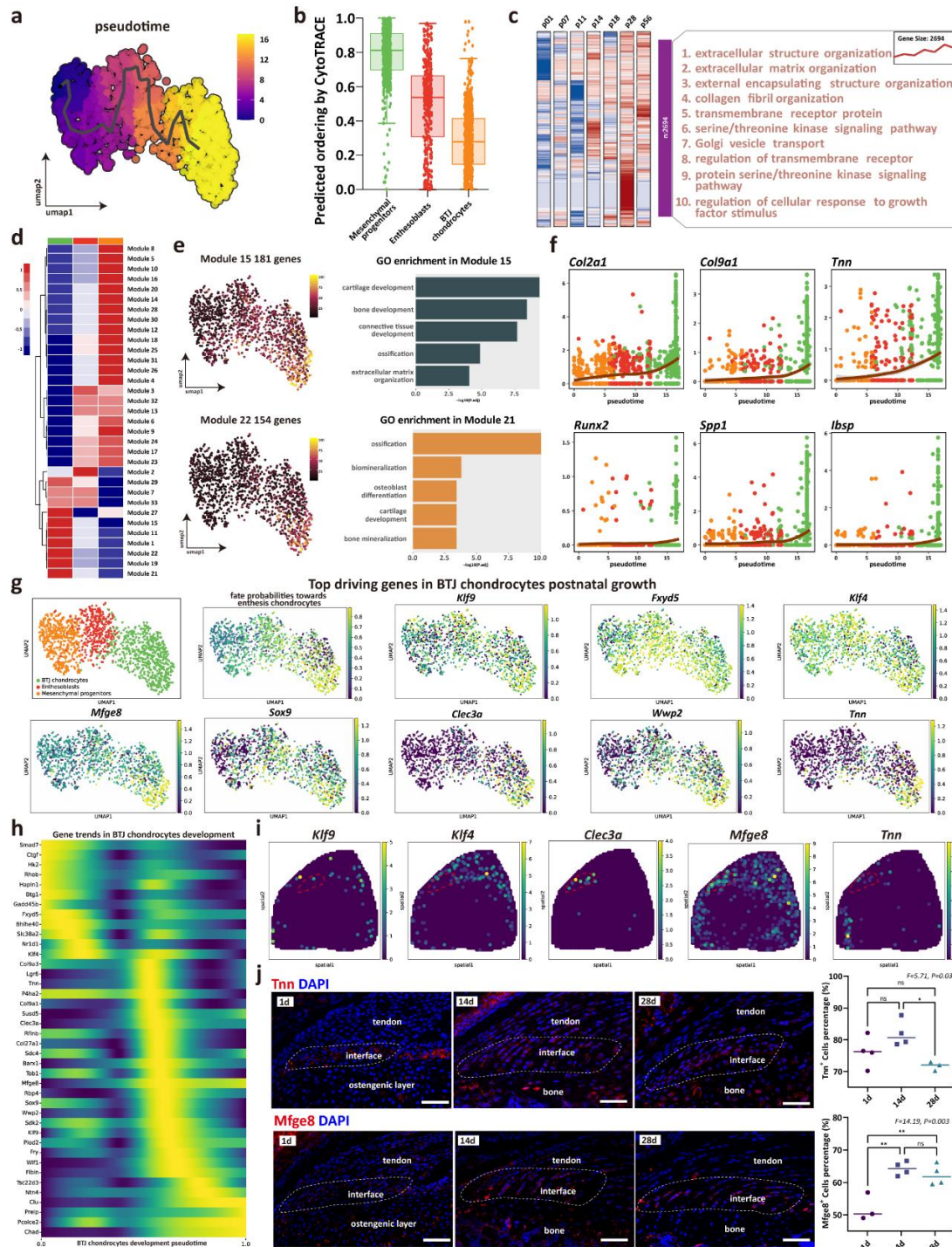


**Figure 2 The trajectory and gene dynamics in BTJ chondrocytes differentiation.** (A) Pseudotime analysis of the three clusters of mesenchymal progenitors, enthesoblasts, and enthesis chondrocytes. (B) Cytotrace scores and predicted ordering of the three subclusters. (C) Heatmap revealing the scaled expression of DEGs and their annotated function for each timepoint. (D) Heatmap showing the modules of coregulated genes grouped by Louvain community analysis. (E) UMAP plots and functional annotation of the representative gene modules, showing the top 5 GO annotations of indicated biological process among each timepoint. (F) Line plots showing representative genes trends in module 15 and 22, respectively. (G) Feature plots showing top driving genes in BTJ chondrocytes growth. (H) Heatmap showing the gene expression dynamics along differentiation trajectories of BTJ chondrocytes. (I) Spatial transcriptomic spot map revealing the expression of driving genes in each spatial spot. (J) Immunofluorescence showing distribution and dense level of Tnn and Mfge8 during different postnatal time. Scale bars, 100  $\mu$ m. \* =  $P < 0.05$ , \*\* =  $P < 0.01$ .

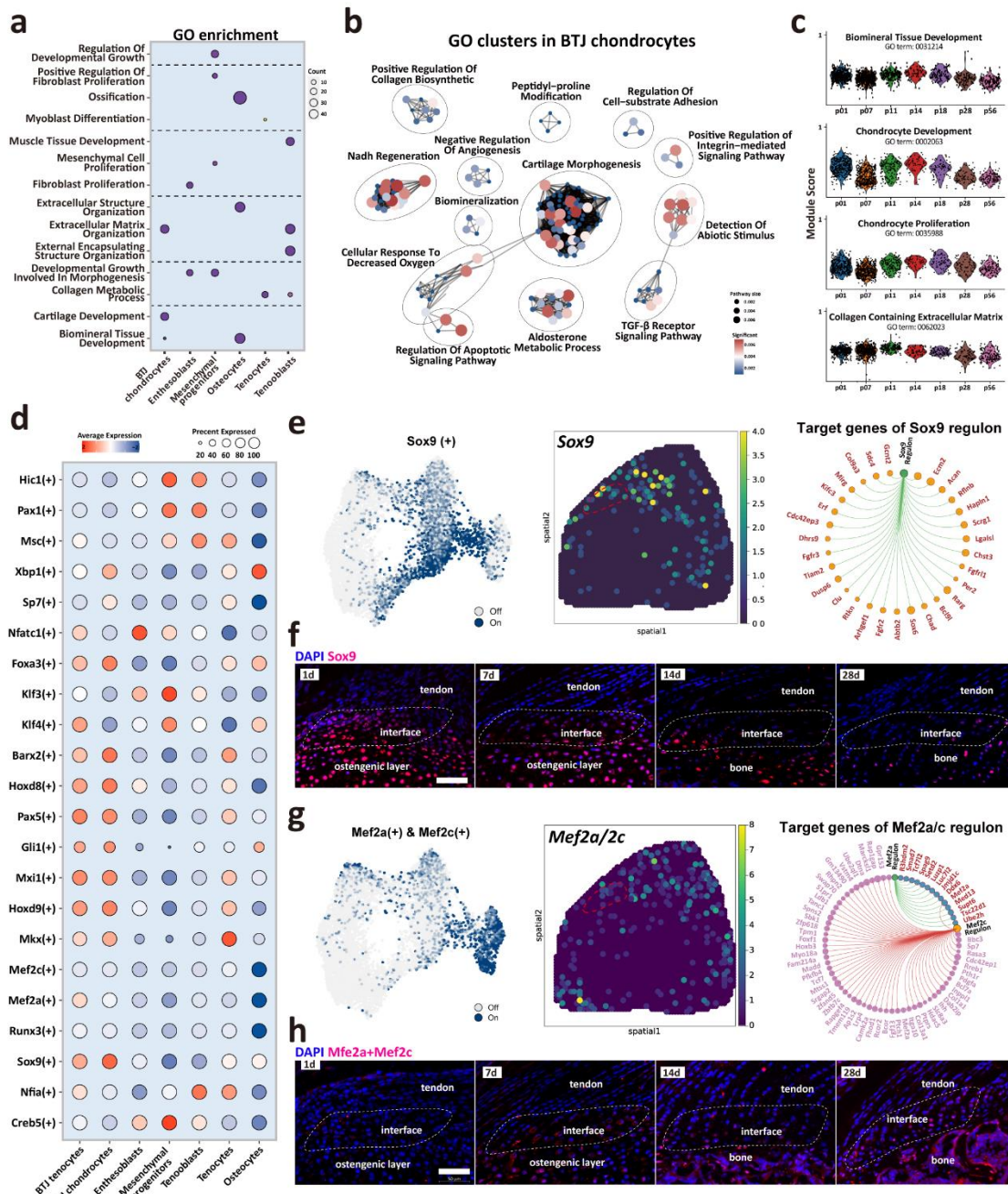


**Figure 3 Biological processes and regulators governing enthesis chondrocytes differentiation.** (A) Heatmap shows the typical biological processes enriched in each cellular cluster. (B) Dot plots show the GO clusters in BTJ chondrocytes in enthesis development. (C) Time-dependent analysis of GO annotations including chondrocyte proliferation, development, and biomineral tissue development decreased with time increased. (D) Heatmap shows the most significant regulatory regulons in each subcluster. (E, G) UMAP plots and spatial expression of Sox9 and Mef2a/Mef2c regulons and their target genes in enthesis chondrocytes. (F, H) Immunofluorescence showing distribution and dense level of Sox9 and Mef2a/Mef2c during different postnatal time. Scale bars, 100  $\mu$ m.